

Measurements of
Inclusive b-quark Production at 7 TeV
with the CMS Experiment

P. BELLAN
ON BEHALF OF
THE CMS COLLABORATION

Padova University and INFN – 35131 Padova, Italy

Abstract

Measurements performed by the CMS experiment of the cross section for inclusive b-quark production in proton-proton collisions at $\sqrt{s} = 7$ TeV are presented. The measurements are based on different methods, such as inclusive jet measurements with secondary vertex tagging or selecting a sample of events containing jets and at least one muon, where the transverse momentum of the muon with respect to the closest jet axis discriminates b events from the background. The results are compared with predictions based on perturbative QCD calculations at leading and next-to-leading order.

PRESENTED AT

Hadron 2011
Munich, Deutschland
June 13–17, 2011

1 Introduction

The study of heavy-quark production in high-energy hadronic interactions plays a key role in testing next-to-leading order (NLO) Quantum Chromodynamics (QCD) calculations. In the past, discrepancies were observed between experimental data and theoretical predictions, e.g. at Tevatron [1, 2, 3, 4] and HERA [5, 6, 7, 8]. Substantial progress has been achieved in the understanding of heavy-quark production at Tevatron energies [9], but large theoretical uncertainties still remain, mainly due to the dependence of the calculations on the renormalization and factorization scales. The observed large scale dependence of the NLO calculations is considered to be a symptom of large contributions from higher orders: small- x effects [10, 11], where $x \sim m_b/\sqrt{s}$, are possibly relevant in the low transverse momentum (p_T) domain, while multiple-gluon radiation leads to large logarithms of p_T/m_b and may be important at high p_T [12]. The resummed logarithms of p_T/m_b at next-to-leading-logarithmic accuracy have been matched to the fixed-order NLO calculation for massive quarks [13]. At the non-perturbative level, the b-hadron p_T spectrum depends strongly on the parametrization of the fragmentation function [14]. The b-quark production cross section has also been studied in the general-mass variable-flavor-number scheme [15] and the k_T factorization QCD approach [16, 17].

Measurements of b-hadron production at higher energies than before, provided by the Large Hadron Collider (LHC), represent an important test of the new theoretical calculations just mentioned. Measurements of inclusive b-quark production cross section require identification of inclusive events in which a b-quark has been produced in pp collisions. In results reported here, the discrimination of the heavy quark events has been achieved either exclusively, reconstructing the whole decay channel of a B meson, or inclusively, considering hard jets. In this context, two different tagging techniques have been applied: reconstruction of a displaced secondary vertex, and analysis of the transverse momentum spectrum of an energetic muon with respect to the closest jet.

2 The CMS detector

A detailed description of the CMS detector can be found elsewhere [18]. Some of the most relevant features for heavy flavor physics are summarized here.

The core CMS apparatus is a superconducting solenoid, of 6 m internal diameter, providing a magnetic field of 3.8 T. Within the field volume there are the silicon pixel and strip tracker, the crystal electromagnetic calorimeter and the brass/scintillator hadron calorimeter. Muons are detected by three types of gas-ionization detectors embedded in the steel return yoke: Drift Tubes (DT), Cathode Strip Chambers (CSC), and Resistive Plate Chambers (RPC). The muon detectors cover a pseudorapidity

window $|\eta| < 2.4$, where $\eta = -\ln[\tan(\theta/2)]$, where the polar angle θ is measured from the z -axis, which points along the counterclockwise beam direction. The silicon tracker is composed of pixel detectors (three barrel layers and two forward disks on each side of the detector, made of 66 million $100 \times 150 \mu\text{m}^2$ pixels) followed by microstrip detectors (ten barrel layers plus three inner disks and nine forward disks on each side of the detector, with 10 million strips of pitch between 80 and $184 \mu\text{m}$). Thanks to the strong magnetic field and the high granularity of the silicon tracker, the transverse momentum, p_T , of the muons matched to reconstructed tracks is measured with a resolution of about 1 % for the typical muons used in this analysis. The silicon tracker also provides the primary vertex position, with $\sim 20 \mu\text{m}$ accuracy.

The first level (L1) of the CMS trigger system, composed of custom hardware processors, uses information from the calorimeters and muon detectors to select the most interesting events. The High Level Trigger (HLT) further decreases the rate before data storage.

3 Open beauty

b-jets play a key role in searches for new physics beyond the Standard Model. It took a while to fully establish a consistency between the Tevatron data and pQCD predictions for b-jet production cross section. Generally speaking, b-jets cross section measurements are highly non-trivial, and sizable uncertainties affect both theory and experiment: on one side, one has to deal with a typical multi-scale problem, in which the center-of-mass collision energy, mass of the b-quark and the factorization and re-normalization scales are entangled in a subtle way; on the other hand, excellent performance of the tracking is required, challenging the detector full potential.

The CMS Collaboration has published results, reviewed in the next sections, concerning two complementary measurements of b-jet production cross section. These results have made use of two different b-tagging techniques, were performed over 85 nb^{-1} and 60 nb^{-1} of 2010 data, respectively [19, 20], and were obtained using track or particle-flow jets. Typical values achieved by the CMS detector of the jet resolution and the energy scale uncertainty, at the time of these results were reported, were about 10 – 15%, and below 3%, respectively.

3.1 b-jets with muons

The measurement of the integrated and differential cross section of the reaction $pp \rightarrow b + X \rightarrow \mu + X$ has been performed on jets coming from b-quarks. The production of a b-quark decaying semi-leptonically is deduced by the identification of a rather energetic muon inside a jet, where the transverse momentum relative to the jet axis is quite sizable. For a muon from a b-decay, the transverse momentum relative to the jet

axis is on average larger than when the muon comes from light quarks; through this property it is hence possible to discriminate events in which b -quarks were produced.

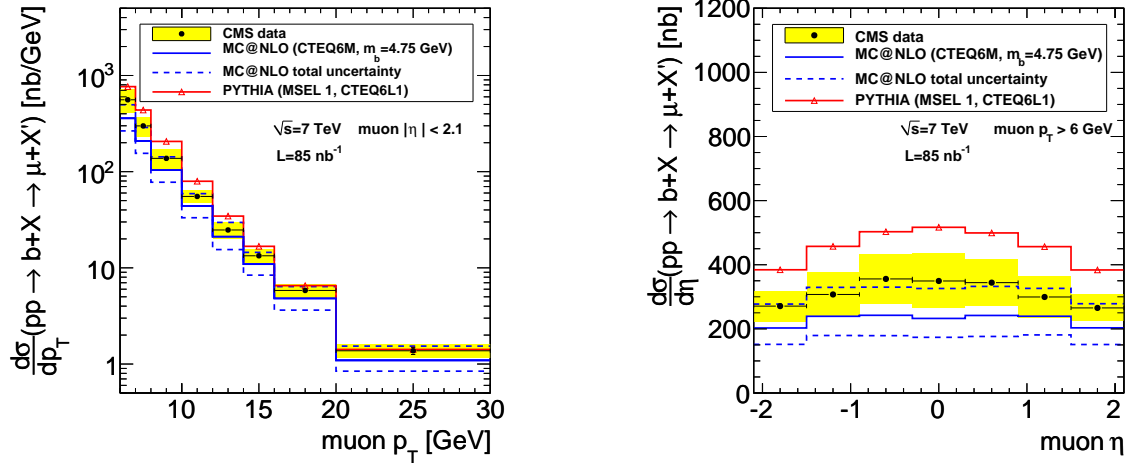


Figure 1: Differential cross section (left) $\frac{d\sigma}{dp_T^\mu}(pp \rightarrow b + X \rightarrow \mu + X', |\eta^\mu| < 2.1)$, and (right) $\frac{d\sigma}{d\eta^\mu}(pp \rightarrow \pm X \rightarrow \mu + X', p_T^\mu > 6 \text{ GeV})$. The two possible muon charges are not distinguished and the process $pp \rightarrow \bar{b} + X \rightarrow \mu + X'$ is included. The black points are the CMS measurements. Vertical error bars showing the statistical error are smaller than the point size in most bins, the horizontal bars indicate the bin width. The yellow band shows the quadratic sum of statistical and systematic uncertainties. The systematic uncertainty (11%) of the luminosity measurement is not included. The solid blue line shows the MC@NLO result and the dashed blue lines illustrate the theoretical uncertainty as described in the text. The solid red line with dots shows the PYTHIA result.

A binned log-likelihood fit is performed on the spectrum of such a quantity, called “ p_T^{rel} ”, using template distributions provided by the simulation for b and c quarks, and derived from the data for gluons and lighter quarks. This latter distribution is dominated by hadrons misidentified as muons (mainly decay-in-flight), so they are reweighted by the misidentification rate measured in the data. Considering that the fit is not able to distinguish between light quark, gluon and charm components, these are merged together. The b -jet tag efficiency achieved with this technique is about 74% at $p_T^\mu \simeq 6 \text{ GeV}$, and close to 100% above 20 GeV, whereas the contamination is $\sim 7\%$ in lowest p_T bin, asymptotically decreasing towards 2% at high p_T .

The result of the inclusive production cross section for b quarks decaying into

muons within the kinematic range $p_T^\mu > 6$ GeV and $|\eta^\mu| < 2.1$ is:

$$\sigma = 1.32 \pm 0.01(\text{stat}) \pm 0.30(\text{syst}) \pm 0.15(\text{lumi}) \mu b$$

where the first uncertainty is statistical, the second is systematic, and the third is associated with the estimation of the integrated luminosity. Fig. 1 shows the measured value of the cross section for the reaction $pp \rightarrow b + X \rightarrow \mu + X$, as a function of the muon's p_T and y . The result includes efficiency of trigger $(88 \pm 5)\%$, of muon reconstruction $(94 \pm 3)\%$ and muon-jet association $(77 \pm 8)\%$.

The fit stability was tested against variation of the binning, repeating the fits on many simulated pseudo-experiments, cross-checking the results using jets from particle flow and performing the fits on the impact parameter distribution.

Table 1: Summary of systematic cross section uncertainties. The systematic uncertainty can vary depending on the muon transverse momentum and pseudorapidity as indicated by the range.

source	cross section uncertainty (%)
Trigger efficiency	5
Muon reconstruction efficiency	3
Hadron tracking efficiency	2
b p_T^{rel} shape uncertainty	≤ 21
Background p_T^{rel} shape uncertainty	2–14
Background composition	3–6
Production mechanism	2–5
Fragmentation	1–4
Decay	3
Underlying event	10
Luminosity	11

Table 1 summarizes the systematic uncertainties entailed in this measurement. The uncertainties dominating the measurement are those coming from the approximate knowledge of the signal and the background p_T^{rel} shape.

Fig. 2 shows the ratio of the measured differential production cross sections in p_T and η over the predictions of the MC@NLO computation, as well as those provided by the Pythia [21], CASCADE MC [22] and the FONLL [23] calculations.

3.2 b-tagging with secondary vertices

The identification of jets coming from the hadronization of b-quarks is possible also through the reconstruction of secondary vertices (SV). Once a displaced SV is re-

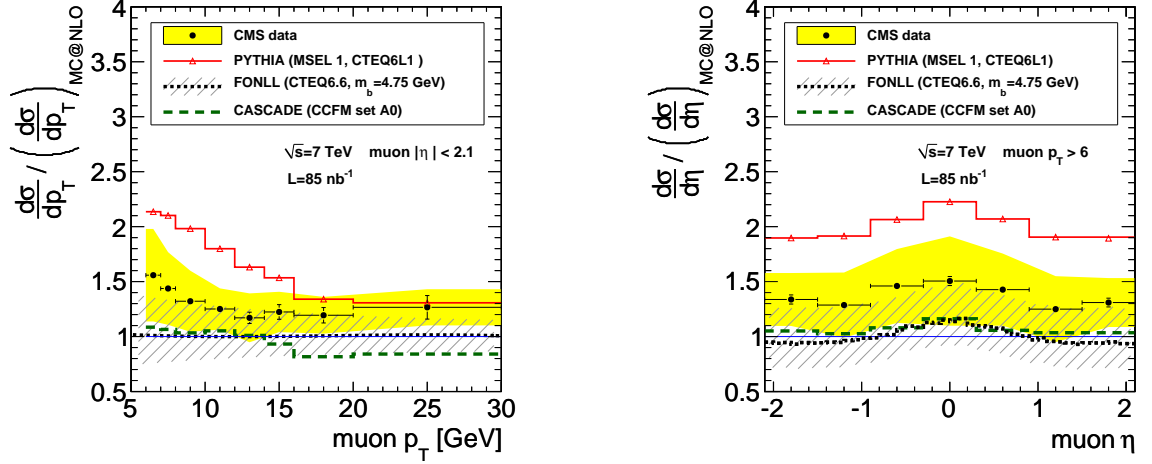


Figure 2: Differential cross section (left) $\frac{d\sigma}{dp_T^\mu}(pp \rightarrow b + X \rightarrow \mu + X', |\eta^\mu| < 2.1)$, and (right) $\frac{d\sigma}{d\eta^\mu}(pp \rightarrow b + X \rightarrow \mu + X', p_T^\mu > 6 \text{ GeV})$, divided by their MC@NLO predictions. The two possible muon charges are not distinguished; the cross section includes the process $pp \rightarrow \bar{b} + X \rightarrow \mu + X$. The black points are the CMS measurements. Vertical error bars showing the statistical error are smaller than the point size in most bins, the horizontal bars indicate the bin width. The yellow band shows the quadratic sum of statistical and systematic uncertainties. The systematic uncertainty (11%) of the luminosity measurement is not included. Superimposed are the FONLL result (black dotted line) with uncertainties (hatched band), the CASCADE result (green, dashed line) and the pythia result (red line with markers), divided by the MC@NLO cross section.

constructed, different discriminators can be used to tag the jet as originating from a b-quark. In the analysis presented here, the discriminator adopted is a monotonic function of the 3D decay length. The decay length significance cut is chosen so that the corresponding tagging efficiency is about 60% at $p_T^{jet} = 100 \text{ GeV}$, with a contamination of $\sim 0.1\%$. The b-tagging efficiency and the mistag rates from c or light jets are evaluated from simulated events and constrained by a data/MC scale factor. The b-tagging efficiency with the selections used in this analysis is between 6% and 60% at $p_T > 18 \text{ GeV}$ and $|y| < 2.0$. The efficiency rises at higher p_T as the b-hadron proper-time increases. In order to evaluate the purity of the selected sample, a fit to the SV mass distribution is performed, taking the shapes from simulated events, and letting free the relative normalizations for c and b jets, with the (small) contribution from light quarks fixed to the Monte Carlo expectations (“template fit”). The efficiencies estimated from MC, and the estimates of b-tagged sample purity resulting from fits to secondary-vertex mass from data are shown in Fig. 3.

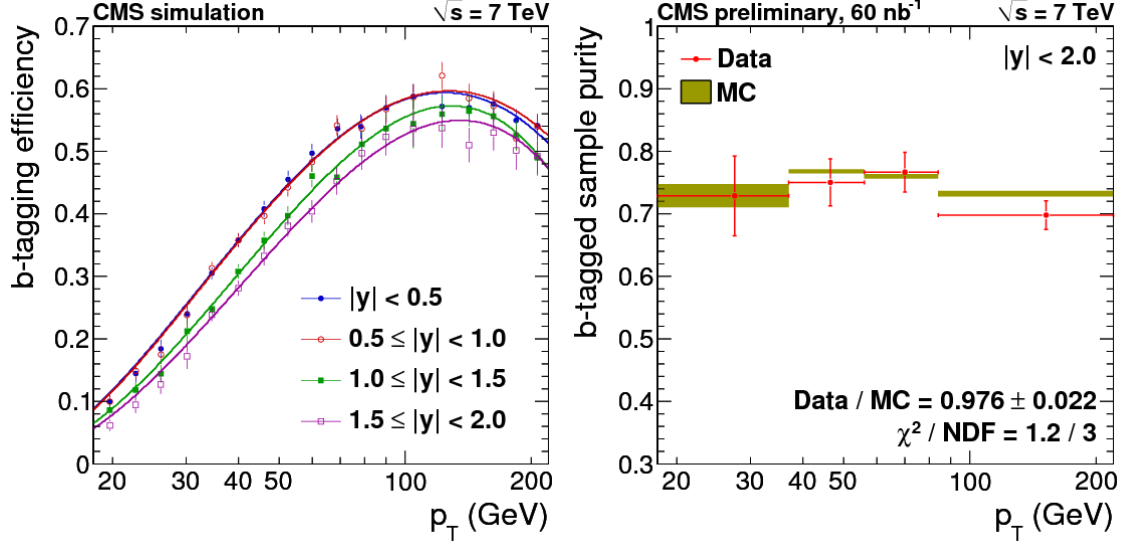


Figure 3: b-tagging efficiency in different rapidity bins, as estimated on simulated events (left). The b-tagged sample purity obtained using fits to secondary vertex mass (right)

The data sample was collected using hadronic triggers with different thresholds of the jet p_T . To merge them, the individual p_T spectra of jets have been normalized with the luminosity of their data taking periods, and then combined into a single spectrum with the jet p_T bins corresponding to intervals where the triggers were fully efficient. The overall transverse jet energy range goes from 18 to 300 GeV, and the measurements have been performed in four η intervals. The jet energy corrections applied for rapidity dependence, and those for absolute scale and p_T dependence, come from real data and simulated events, respectively.

The leading systematic uncertainties affecting the measurements are:

- the jet energy scale of b-jets relatively to the inclusive ones (45%);
- data-driven constraints on b-tagging efficiency (20%);
- mistag rate for charm (34 %) and for light jets (1 - 10%).

Fig. 4 shows the results for the production cross section measurements for b-jets as a function of the b-jet transverse momentum, compared with the MC@NLO predictions, and the ratio with the inclusive jets cross-section. While the agreement with Pythia and MC@NLO is reasonable, significant differences in shape are evident, the simulations predicting more b-jets at high p_T than what is observed.

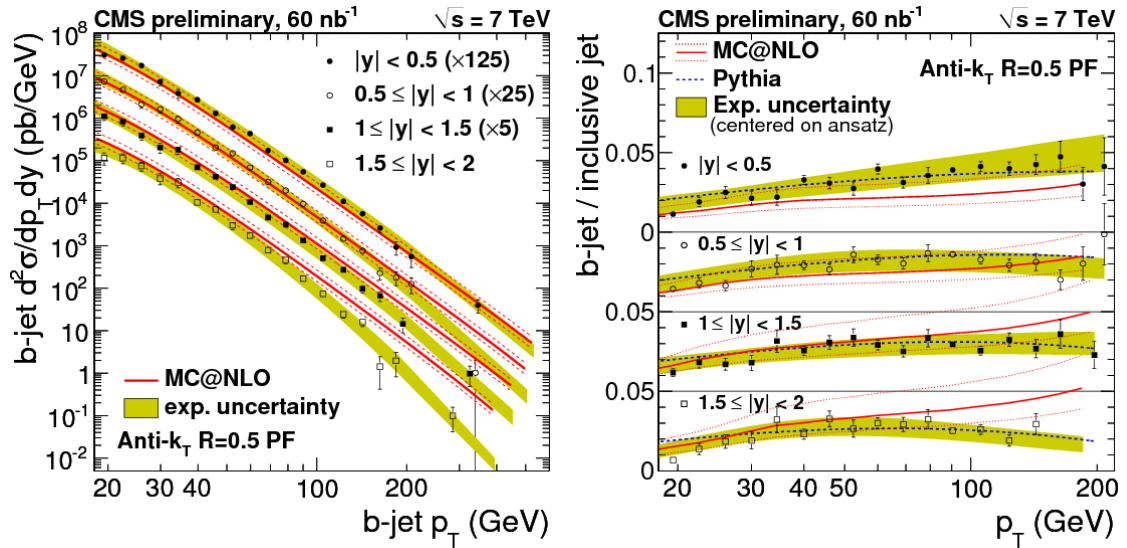


Figure 4: Production cross section measurement for b-jet as a function of the b-jet transverse momentum compared with the MC@NLO predictions (left) and the ratio of the b-jet cross section over the inclusive jets (right).

4 Conclusions

Recent results published by the CMS Collaboration on open beauty production have been summarized, all of them obtained analyzing the pp collision data at 7 TeV collected in the year 2010. The studies made with two different techniques for b-tagging have been shown, together with the comparisons of the production cross section measured in the data with the predictions from the available theoretical models.

ACKNOWLEDGEMENTS

The involvement in this work was made possible by the founding of the INFN, sezione di Padova. I am grateful to Prof. U. Gasparini for all the sustaining and encouraging, and to the entire CMS Padova group for the fruitful collaboration.

References

- [1] D0 Collaboration, “Inclusive μ and b quark production cross-sections in $p\bar{p}$ collisions at $\sqrt{s} = 1.8$ TeV”, Phys. Rev. Lett. 74 (1995) 35483552.
- [2] D0 Collaboration, “The $b\bar{b}$ production cross section and angular correlations in $p\bar{p}$ collisions at $\sqrt{s} = 1.8$ TeV”, Phys. Lett. B487 (2000) 264272.

- [3] CDF Collaboration, “Measurement of the bottom quark production cross section using semileptonic decay electrons in $p\bar{p}$ collisions at $\sqrt{s} = 1.8$ TeV”, Phys. Rev. Lett. 71 (1993) 500504.
- [4] CDF Collaboration, “Measurement of the b-Hadron Production Cross Section Using Decays to $\mu D_0 X$ Final States in $p\bar{p}$ Collisions at $\sqrt{s} = 1.96$ TeV”, Phys. Rev. D79 (2009) 092003.
- [5] H1 Collaboration, “Measurement of open beauty production at HERA”, Phys. Lett. B467 (1999) 156164.
- [6] H1 Collaboration, “Measurement of beauty production at HERA using events with muons and jets”, Eur. Phys. J. C41 (2005) 453467.
- [7] ZEUS Collaboration, “Measurement of beauty photoproduction using decays into muons in dijet events at HERA”, JHEP 04 (2009) 133.
- [8] ZEUS Collaboration, “Measurement of charm and beauty production in deep inelastic ep scattering from decays into muons at HERA”, Eur. Phys. J. C65 (2010) 6579.
- [9] M. Cacciari, S. Frixione, M. L. Mangano et al., “QCD analysis of first b cross-section data at 1.96 TeV”, JHEP 0407 (2004) 033.
- [10] J.C. Collins and R.K. Ellis, “Heavy quark production in very high-energy hadron collisions”, Nucl. Phys. B 360 (1991) 3.
- [11] S. Catani, M. Ciafaloni and F. Hautmann, “High-energy factorization and small x heavy flavor production”, Nucl. Phys. B 366 (1991) 135.
- [12] M. Cacciari and M. Greco, “Large p_T hadroproduction of heavy quarks”, Nucl. Phys. B 421 (1994) 530.
- [13] M. Cacciari, M. Greco and P. Nason, “The p_T spectrum in heavy- flavour hadroproduction”, JHEP 05 (1998) 007.
- [14] S. Frixione et al., “Heavy quark production”, Adv. Ser. Direct. High Energy Phys. 15 (1998) 609.
- [15] B.A. Kniehl, G. Kramer, I. Schienbein and H. Spiesberger, “Finite-mass effects on inclusive B-meson hadroproduction”, Phys. Rev. D 77 (2008) 014011.
- [16] M.G. Ryskin, A.G. Shuvaev and Y.M. Shabelski, “Comparison of k_T factorization approach and QCD parton model for charm and beauty hadroproduction”, Phys. Atom. Nucl. 64 (2001) 1995.

- [17] H. Jung, “Heavy quark production at the Tevatron and HERA using k_T factorization with CCFM evolution”, Phys. Rev. D 65 (2002) 034015.
- [18] CMS Collaboration, “The CMS experiment at the CERN LHC”, JINST 0803 (2008) S08004.
- [19] CMS Collaboration, “Inclusive b-hadron production cross section with muons in pp collisions at $\sqrt{s} = 7$ TeV”, Journal of High Energy Physics Volume 2011, Number 3, 90.
- [20] CMS Collaboration, “Inclusive b-jet production in pp collisions at $\sqrt{s} = 7$ TeV”, CMS-PAS-BPH-10-009.
- [21] T. Sjöstrand, S. Mrenna, P.Z. Skands, “PYTHIA 6.4 physics and manual”, J. High Energy Phys. 0605, 026 (2006).
- [22] H. Jung et al., “The CCFM Monte Carlo generator CASCADE”, Comput. Phys. Commun. 143 (2002) 100-111.
- [23] M. Cacciari, S. Frixione, P. Nason, “The p_T spectrum in heavy flavor photoproduction”, J. High Energy Phys. 0103, 006 (2001).